RIS-mounted UAV for Cell-Free ISAC Network: Joint Beamforming and Localization Optimization

Shanza Shakoor[‡], Quang Nhat Le[‡], and Trung Q. Duong[‡]
[‡]Memorial University, Canada (e-mail: {sshakoor, qnle, tduong}@mun.ca)

***Abstract*—This paper considers the cell-free integrated sensing and communication (CF-ISAC) networks utilizing reconfigurable intelligent surface (RIS)-mounted unmanned aerial vehicles (UAVs). We aim to maximize the weighted sum rate by jointly optimizing access points (APs)' transmit beamformings, RISs' phase shifts, user-RIS association, and UAVs' locations. Since the formulated problem is non-convex, it is decomposed into three subproblems. For optimizing APs' transmit beamforming, RISs' phase shifts and user-RIS association, we convert the log-sum problem into a quadratically constrained quadratic programming problem using the Lagrangian dual principle and multi-ratio fractional programming. For optimizing UAVs' locations, the successive convex approximation technique is used to transform it into a convex problem. Simulation results highlight the considerable performance advantage of the proposed network compared to benchmark schemes.**

I. Introduction

The rapid advancement of wireless communication and the development of 6G networks demand high data rates, ultra-low latency, and intelligent network adaptability [1]. Integrated sensing and communication (ISAC) addresses these needs by enabling simultaneous communication and environmental sensing within the same frequency bands and hardware resources [2], [3]. ISAC improves spectrum efficiency, reduces infrastructure costs, and enhances situational awareness, making it essential for autonomous systems, smart cities, and next-generation vehicular networks [4]. However, achieving seamless joint communication and sensing in dynamic environments requires advanced network architectures to optimize performance [5].

Traditional cellular networks, reliant on centralized base stations, encounter coverage limitations, interference, and unreliable sensing in non-line-of-sight (NLoS) environments [6]. To tackle these challenges, cell-free ISAC (CF-ISAC) networks have been introduced as a distributed solution, where multiple access points (APs) collaborate to serve users and perform sensing tasks without cell boundaries, improving coverage, spectral efficiency, and localization accuracy [7], [8]. However, optimizing joint beamforming and localization in CF-ISAC networks remains challenging due to dynamic environments, interference, and resource allocation constraints.

To further enhance communication reliability and sensing precision in CF-ISAC networks, reconfigurable intelligent surface (RIS) has been introduced as a key enabler for next-generation wireless systems. RIS, consisting of passive, programmable meta-surfaces, improves signal strength and coverage in challenging environments [9], [10]. For instance, [11] explores joint optimization of beamforming and RIS's phase shifts, while [12] investigates dual-functional RIS for target detection and communication. However, static RIS deployment is often limited by environmental and infrastructure factors, which motivates the integration of RIS with unmanned aerial vehicle (UAV) for increased flexibility and adaptability [13].

The integration of RIS-mounted UAV (URIS) into CF-ISAC networks offers advantages like dynamic 3D beamforming, optimizing UAV positions and RIS configurations to enhance coverage and communication efficiency [14]. UAV with RIS act as additional sensing nodes, improving localization accuracy through superior LoS conditions and adaptive repositioning based on user demands and environmental dynamics [15], [16]. However, effectively using URIS requires intelligent user association to balance communication and sensing performance while minimizing interference [17]. Studies like [14] demonstrate the benefits of optimizing UAV positioning and RIS's phase shifts, and [15] explores energy-efficient deployment strategies.

Despite these advancements, existing research lacks comprehensive solutions for joint optimization of beamforming, UAV's trajectory, and interference management in dynamic CF-ISAC networks, particularly under real-time topology changes and dense deployments. To address these gaps, this paper proposes an URIS-assisted framework that jointly optimizes APs' transmit beamformings, RISs' phase shifts, UAVs placement, and user-RIS association by leveraging successive convex approximation (SCA) for UAVs positioning and multi-ratio fractional programming to effectively optimize both APs' transmit beamformings and RISs' phase shifts. Furthermore, a penalty-based user-RIS association strategy is proposed to reduce channel training overhead, thereby improving scalability. Simulation results validate the framework's effectiveness in improving weighted sum rate in dynamic CF-ISAC networks.

II. System Model

As illustrated in Fig. 1, we consider a system comprising multiple URISs to enhance the communication quality within a CF-ISAC network. The system includes a set of $\mathcal{L} = \{1, \ldots, L\}$ APs, $\mathcal{F} = \{1, \ldots, F\}$ sensing receivers

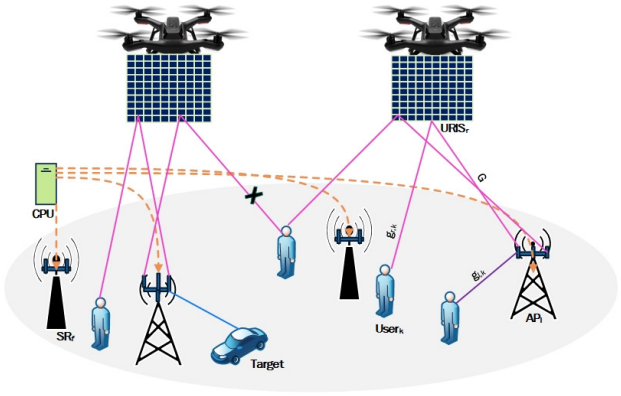

Fig. 1. The system model of CF-ISAC network with URISs.

(SRs), $\mathcal{R} = \{1, \ldots, R\}$ RISs, $\mathcal{K} = \{1, \ldots, K\}$ users, and a single sensing target. Each AP is equipped with $\mathcal{M} = \{1, \ldots, M\}$ transmitter/receiver antennas arranged as a uniform linear array (ULA) to transmit communication–radar signals and receive echo signals, while each RIS consists of $\mathcal{N} = \{1, \ldots, N\}$ reflecting elements to improve the communication link from the APs to a single-antenna users. All APs are connected to a central server via high-speed wired links, while the UAVs and RIS communicate wirelessly with the central server, forming a unified and high-performance network infrastructure.

The UAV and RIS act as a single entity for simplicity and the impact of the RIS's size and weight on the solution is neglected. The URIS is only permitted to fly in area E. The spatial locations of $l-$th AP, $k-$th user, target and $r-$th URIS can be denoted as $\boldsymbol{\chi}_l^L = (x_l^L, y_l^L)^T$, $\boldsymbol{\chi}_k^K = (x_k^K, y_k^K)^T$, $\boldsymbol{\chi}_0 = (x_0, y_0)^T$, and $\mathbf{q}_r^R = (x_r^R, y_r^R)^T$. The height of $k-$th user, target, $l-$th APs and $r-$th URIS is denoted as h_k, h_o, h_l and h_r, respectively. The distance between the $r-$th URIS and $l-$th AP, $k-$th user and target is denoted by

$$d_{lr} = \sqrt{\|\mathbf{q}_r^R - \boldsymbol{\chi}_l^L\|^2 + |h_r - h_l|^2}, \tag{1}$$

$$d_{ro} = \sqrt{\|\mathbf{q}_r^R - \boldsymbol{\chi}_0\|^2 + |h_r - h_0|^2}, \tag{2}$$

$$d_{rk} = \sqrt{\|\mathbf{q}_r^R - \boldsymbol{\chi}_k^K\|^2 + |h_r - h_k|^2}. \tag{3}$$

A. Transmission Model

The complex baseband signal transmitted by $l-$th AP is represented as

$$\mathbf{x}_l = \sum_{k \in \mathcal{K}} \mathbf{w}_{l,k} s_k + \mathbf{w}_{l,0} s_0, \tag{4}$$

where $\mathbf{w}_{l,k} \in \mathbb{C}^{M \times 1}$ and $\mathbf{w}_{l,0} \in \mathbb{C}^{M \times 1}$ denote the beamforming vectors for transmitting data to $k-$th user and sensing stream to target, respectively, with s_k and s_0 representing the associated $k-$th user's data and sensing stream.

B. Channel Model

We consider a 2D Cartesian coordinate system with URISs at fixed altitudes. The AP-user link consists of both LOS and URIS-assisted NLOS paths, while the AP-target link is restricted to direct LOS communication. The channel gains between the $l-$th AP-$r-$th RIS, $r-$th RIS-$k-$th user and $l-$th AP-$k-$th user are denoted by $\mathbf{G}_{l,r} \in \mathbb{C}^{N \times M}$, $\mathbf{g}_{r,k} \in \mathbb{C}^{N \times 1}$, and $\mathbf{g}_{l,k}, \in \mathbb{C}^{M \times 1}$, respectively, which are shown as

$$\mathbf{G}_{l,r} = \sqrt{\alpha d_{lr}^{-2}} \left(\sqrt{\frac{\beta}{\beta+1}} \mathbf{G}_{lr}^{\text{LoS}} + \sqrt{\frac{1}{\beta+1}} \mathbf{G}_{lr}^{\text{NLoS}} \right), \tag{5}$$

$$\mathbf{g}_{r,k} = \sqrt{\alpha d_{rk}^{-2}} \left(\sqrt{\frac{\beta}{\beta+1}} \mathbf{g}_{rk}^{\text{LoS}} + \sqrt{\frac{1}{\beta+1}} \mathbf{g}_{rk}^{\text{NLoS}} \right), \tag{6}$$

$$\begin{aligned} \mathbf{g}_{l,k} &= \sqrt{\alpha d_{lk}^{-2}} \left(\sqrt{\frac{\beta}{\beta+1}} \mathbf{g}_{lk}^{\text{LoS}} + \sqrt{\frac{1}{\beta+1}} \mathbf{g}_{lk}^{\text{NLoS}} \right), \\ &= \sqrt{\alpha d_{lk}^{-2}} \mathbf{g}_{lk}^{\text{LoS}}, \end{aligned} \tag{7}$$

where α and β represent the path loss per unit distance and the Rician factor, respectively. $\mathbf{G}_{lr}^{\text{NLoS}}$ and $\mathbf{g}_{rk}^{\text{NLoS}}$ represent the NLoS channel components, which follow the Gaussian distribution. The LOS component of the $\mathbf{G}_{l,r}$ channel is given as $\mathbf{G}_{lr}^{\text{LoS}} = \mathbf{a}_r^H(\theta_{r,l}, \phi_{r,l}) \mathbf{a}_l(\theta_{l,r}, \phi_{l,r})$. where $\theta_{l,r}$ and $\phi_{l,r}$ represents the elevation and azimuth angles, respectively. The spatial parameters are calculated as $\sin(\theta_{l,r}) \sin(\phi_{l,r}) = \frac{y_r^R - y_l^L}{d_{lr}}$, $\cos(\theta_{l,r}) = \frac{h_r - h_l}{d_{lr}}$, $\sin(\theta_{r,l}) \cos(\phi_{r,l}) = \frac{x_l^L - x_r^R}{d_{lr}}$, and $\sin(\theta_{r,l}) \sin(\phi_{r,l}) = \frac{y_l^L - y_r^R}{d_{lr}}$.

C. Communication Model

For each user, the signal transmitted from the APs can propagate through two distinct paths: the direct AP-to-user link and the indirect AP-to-RIS-to-user link, where the RIS enhances connectivity by reflecting the signal towards the user. To model the association between users and RISs, let $u_{k,r} \in \{0, 1\}$ indicate whether k-th user is associated with r-th RIS or not. The association vector for k-th user, representing its connection to all RISs, is given as $\mathbf{u}_k = [u_{k,1}, \ldots, u_{k,R}]^T$. For all users and RISs, the association matrix is represented as $\mathcal{U} = [\mathbf{u}_1, \ldots, \mathbf{u}_K]^T \in \mathbb{R}^{K \times R}$. Therefore, the signal received by k-th user is expressed as

$$\mathbf{y}_k = \sum_{l \in \mathcal{L}} \sum_{r \in \mathcal{R}} (\mathbf{g}_{l,k}^H + u_{k,r} \mathbf{g}_{r,k}^H \boldsymbol{\Theta}_r \mathbf{G}_{l,r}) \mathbf{x}_l + n_k, \tag{8}$$

where $n_k \sim \mathcal{CN}(0, \sigma^2)$ denotes the additive white Gaussian noise (AWGN) with variance σ_k^2 at the k-th user. The phase shift matrix of the $r-$th RIS, represented by $\boldsymbol{\Theta}_r = \text{diag}(e^{j\theta_{r,1}}, \ldots, e^{j\theta_{r,N}}) = \text{diag}(\psi_{r,1}, \ldots, \psi_{r,N})$, defines the phase shift matrix of the $r-$th RIS, where $\theta_{r,n}$ denotes the phase shift of the n-th element. It is assumed that these phase shift values can be continuously tuned within the interval $[0, 2\pi)$. The received signal-to-interference-plus-noise ratio (SINR) at k-th user can expressed as

$$\gamma_k = \frac{|\mathbf{g}_k^H \mathbf{w}_k|^2}{\sum\limits_{j \in \bar{\mathcal{K}} \setminus k} |\mathbf{g}_k^H \mathbf{w}_j|^2 + \sigma_k^2}, \tag{9}$$

where $\hat{\mathbf{g}}_{l,k}^H = (\mathbf{g}_{l,k}^H + u_{k,r}\mathbf{g}_{r,k}^H \mathbf{\Theta}_r \mathbf{G}_{l,r})$, $\bar{\mathcal{K}} = \mathcal{K} \cup \{0\}$, $\mathbf{g}_k = \left[\hat{\mathbf{g}}_{1,k}^H \ldots, \hat{\mathbf{g}}_{L,k}^H\right]^H$, $\mathbf{w} \triangleq \{\mathbf{w}_{l,0}, \mathbf{w}_{l,k}\}_{l\in\mathcal{L},k\in\mathcal{K}}$, $\mathbf{w}_0 = \left[\mathbf{w}_{1,0}^H, \ldots, \mathbf{w}_{L,0}^H\right]^H$, and $\mathbf{w}_k = [\mathbf{w}_{1,k}^H, \ldots, \mathbf{w}_{L,k}^H]^H$. The weighted sum rate of all users can be expressed as

$$\Upsilon = \sum_{k\in\mathcal{K}} \varpi_k \log_2(1+\gamma_k), \tag{10}$$

where ϖ_k denotes the communication weight of k-th user.

D. Sensing Model

We consider multi-static sensing, in which the central server collects and processes signals received from all F SRs for target detection [18]. The signal received by the f-th SR is given by

$$\boldsymbol{y}_f = \sum_{l\in\mathcal{L}} \kappa_{f,l}\sqrt{\Lambda_{f,l}}\boldsymbol{\rho}(\varphi_f)\boldsymbol{\rho}^H(\varphi_l)\boldsymbol{x}_l + n_f, \tag{11}$$

where $\kappa_{f,l} \sim \mathcal{CN}(0, \sigma_{f,l}^2)$ denotes the radar cross section (RCS) of the target from $l-$th AP to f-th SR, $\Lambda_{f,l} = \frac{\lambda_c^2}{(4\pi)^3 d_{f,o}^2 d_{l,o}^2}$ means the channel gain from the $l-$th AP to the sensing target at the distance $d_{l,o}$ and from the target to the f-th SR at the distance $d_{f,o}$, λ_c is the carrier wavelength, $\boldsymbol{\rho}(\varphi)$ denotes the array response vector such that φ_l/φ_f is the angle of departure/arrival from the target location to the $l-$th AP/f-th SR, and $n_f \sim \mathcal{CN}(\mathbf{0}, \sigma^2\mathbf{I}_M) \in \mathbb{C}^{M\times 1}$ is the receiver noise at the f-th SR. By jointly processing the received signal from all SRs, the joint sensing SNR can be derived as

$$\gamma_s = \frac{\sum\limits_{f\in\mathcal{F}}\sum\limits_{l\in\mathcal{L}} \sigma_{f,l}^2 \Lambda_{f,l} ||\boldsymbol{\rho}^H(\varphi_l)\boldsymbol{W}_l||^2}{F\sigma^2}, \tag{12}$$

where $\boldsymbol{W}_l = [\boldsymbol{w}_{l,0}, \boldsymbol{w}_{l,1}, \ldots, \boldsymbol{w}_{l,K}] \in \mathbb{C}^{M\times(K+1)}$ concatenates the beamforming vectors of all UEs and the sensing target.

III. Problem Formulation

Our objective is to maximize the weighted sum rate of all users, through the joint optimization of beamforming $\mathbf{w}$, phase shift Θ, UAV location $\mathbf{q}$ and RIS-user association $\mathcal{U}$. $\mathbf{q} \triangleq \{\mathbf{q}_r^R\}_{r\in\mathcal{R}}$, $\mathbf{\Theta} \triangleq \{\mathbf{\Theta}_r\}_{r\in\mathcal{R}}$. Therefore, the optimization problem can be formulated as

$$\max_{\mathbf{w},\mathbf{\Theta},\mathbf{q},\mathcal{U}} \quad \Upsilon \tag{13a}$$

s.t.

$$\gamma_s \geq \gamma_{th}^{sens}, \tag{13b}$$

$$\|\boldsymbol{w}_{l,0}\|^2 + \sum_{k\in\mathcal{K}} \|\boldsymbol{w}_{l,k}\|^2 \leq P_l^{\max}, \forall l \in \mathcal{L}, \tag{13c}$$

$$|\psi_{r,n}| = 1, \forall r = 1, \ldots R, \forall n = 1, \ldots N, \tag{13d}$$

$$\sum_{r\in\mathcal{R}} u_{k,r} \leq R_{connect}, \forall k \in \mathcal{K}, \tag{13e}$$

$$u_{k,r} \in \{0,1\}, \forall k \in \mathcal{K}, \forall r \in \mathcal{R}, \tag{13f}$$

$$\mathbf{q}_r^R \in E, \forall r \in \mathcal{R}. \tag{13g}$$

Constraints (13b) and (13c) represent the minimum sensing SINR requirement for the target and the maximum transmit power for the $l-$th AP, respectively. Constraint (13e) illustrates the number of RIS with which k-th user can be paired is limited to $R_{connect}$. Problem (13) is non-convex because of the non-concave objective function (13a) and non-convex constraints (13b), (13d), and (13f).

IV. Proposed Solution

A. Transformation of Objective Function

To simplify the objective function (13a), we use the fractional programming (FP) method to convert the objective function into more favorable polynomial expression. As derived in [11], [19], we introduce an auxiliary variable $\mathbf{b} = [b_1, b_2 \ldots, b_K]^T$ to separate the ratio term γ_k in (10) from the logarithmic function via the Lagrangian dual reformulation. This transforms (13a) into a more solvable polynomial form, which can be expressed as

$$\sum_{k\in\mathcal{K}} \varpi_k \log_2(1+b_k) - \sum_{k\in\mathcal{K}} \varpi_k b_k + \sum_{k\in\mathcal{K}} \frac{(1+b_k)\gamma_k}{1+\gamma_k}, \tag{14}$$

where the optimal value of b_k can be obtained by computing the first-order partial derivative of equation (14) with respect to b_k and setting it equal to zero. When this optimal value is found, the objective function in (13a) becomes equivalent to (14). The value of b_k at optimality is therefore determined by

$$b_k^* = \gamma_k. \tag{15}$$

Nevertheless, the final term in (14) remains a complex non-convex fraction. To simplify the solution process, we apply a quadratic transformation [11], [19] to convert it into a more tractable form, which is show as follows:

$$2\sqrt{\varpi_k(1+b_k)}\Re\{\delta_k^* \mathbf{g}_k^H \mathbf{w}_k\} - |\delta_k|^2 \left(\sum_{j\in\bar{\mathcal{K}}\setminus k} |\mathbf{g}_k^H \mathbf{w}_j| + \sigma^2\right), \tag{16}$$

where the optimal value of the relaxation variable δ_k is determined as

$$\delta_k^* = \frac{\sqrt{\varpi_k(1+b_k)}\mathbf{g}_k^H \mathbf{w}_k}{\sum\limits_{j\in\bar{\mathcal{K}}\setminus k} |\mathbf{g}_k^H \mathbf{w}_j| + \sigma^2}. \tag{17}$$

After determining the auxiliary variables b_k and δ_k and applying the corresponding transformations in (14) and (16), the objective function (13a) can be expressed in terms of $\mathbf{w}$ and $\mathbf{\Theta}$ as

$$f(\mathbf{w}, \mathbf{\Theta}, \mathbf{q}, b_k, \delta_k) = \sum_{k\in\mathcal{K}} 2\sqrt{\varpi_k(1+b_k)}\Re\{\delta_k^* \mathbf{g}_k^H \mathbf{w}_k\} - \sum_{k\in\mathcal{K}} |\delta_k|^2 \left(\sum_{j\in\bar{\mathcal{K}}\setminus k} |\mathbf{g}_k^H \mathbf{w}_j| + \sigma^2\right) \tag{18}$$

B. Beamforming Optimization

With fixed $\mathbf{\Theta}, \mathbf{q}, b_k, \delta_k, \mathcal{U}$, the transmit beamforming optimization problem is reduced to

$$\max_{\mathbf{w}} \quad \sum_{k\in\mathcal{K}} 2\sqrt{\varpi_k(1+b_k)}\Re\{\delta_k^* \mathbf{g}_k^H \mathbf{w}_k\} \tag{19a}$$

$$- \sum_{k\in\mathcal{K}} |\delta_k|^2 \left(\sum_{j\in\bar{\mathcal{K}}\setminus k} |\mathbf{g}_k^H \mathbf{w}_j| + \sigma^2 \right)$$

s.t.

$$(13c), (20), \tag{19b}$$

where numerator term of γ_s in the non-convex constraint (13b) is convexified by employing the inequality $||\boldsymbol{\tau}||^2 \geq 2\Re\{(\boldsymbol{\tau}^{(t)})^H \boldsymbol{\tau}\} - ||\boldsymbol{\tau}^{(t)}||^2$, with $\boldsymbol{\tau} = \boldsymbol{\rho}^H(\varphi_l)\boldsymbol{W}_l$. This technique effectively convexifies the numerator term of γ_s. As a result, (13b) is rewritten as

$$\frac{\sum_{f\in\mathcal{F}} \sum_{l\in\mathcal{L}} \sigma_{f,l}^2 \Lambda_{f,l} \big(2\Re\{(\boldsymbol{\tau}^{(t)})^H \boldsymbol{\tau}\} - ||\boldsymbol{\tau}^{(t)}||^2\big)}{F\sigma^2} \geq \gamma_{th}^{sens}. \tag{20}$$

C. Phase Shift and User-RIS Association Optimization

With fixed $\mathbf{w}, \mathbf{q}, b_k, \delta_k$, the RISs' phase shifts and user-RIS association optimization problem can be formulated as

$$\max_{\mathbf{\Theta}, \mathcal{U}} \quad \sum_{k\in\mathcal{K}} 2\sqrt{\varpi_k(1+b_k)}\Re\{\delta_k^\dagger \boldsymbol{\psi}^H \mathbf{g}_{k,k}\} \tag{21a}$$

$$- \sum_{k\in\mathcal{K}} |\delta_k|^2 \left(\sum_{j\in\bar{\mathcal{K}}\setminus k} \boldsymbol{\psi}^H \mathbf{g}_{k,j} \mathbf{g}_{k,j}^H \boldsymbol{\psi} + \sigma^2 \right)$$

s.t.

$$(13d), (13e), (13f), \tag{21b}$$

where

$$\delta_k^\dagger = \frac{\sqrt{\varpi_k(1+b_k)}\boldsymbol{\psi}^H \mathbf{g}_{k,j}}{\sum_{j\in\bar{\mathcal{K}}\setminus k} \boldsymbol{\psi}^H \mathbf{g}_{k,j} \mathbf{g}_{k,j}^H \boldsymbol{\psi} + \sigma^2}, \tag{22}$$

$$\mathbf{g}_{k,j}^H \mathbf{w}_{k,k} = \sum_{l\in\mathcal{L}} \sum_{r\in\mathcal{R}} (\mathbf{g}_{l,k} + \mathbf{u}_k^T \mathbf{g}_{r,k}^H \mathbf{\Theta}_r \mathbf{G}_{l,r}) \mathbf{w}_{l,j} = \boldsymbol{\psi}^H \mathbf{g}_{k,j},$$

$$\mathbf{g}_{k,j}^H = \eta + \mathbf{u}_k^T \boldsymbol{\zeta}_{k,j}, \tag{23}$$

where $\zeta_{k,j,r} = \sum_{l\in\mathcal{L}} \mathbf{g}_{r,k}^H \mathbf{\Theta}_r \mathbf{G}_{l,r} \mathbf{w}_{l,j}$, $\boldsymbol{\zeta}_{k,j} = [\zeta_{k,j,1}, \ldots, \zeta_{k,j,R}]^T$, and $\eta = \sum_{l\in\mathcal{L}} \mathbf{g}_{l,k} \mathbf{w}_{l,j}$. For the binary association between the user-RIS match variable $u_{k,r}$, we first relax (13f) into a continuous variable. Let $\Xi(\mathbf{u}) = \sum_{r\in R} \sum_{k\in K} u_{r,k}$, $\Pi(\mathbf{u}) = \sum_{r\in R} \sum_{k\in K} (u_{r,k})^2$, we impose the following constraints [17]

$$\Xi(\mathbf{u}) - \Pi(\mathbf{u}) \leq 0, \forall r, k, \tag{24}$$

$$0 \leq u_{r,k} \leq 1, \forall r, k. \tag{25}$$

Note that (24) represents a difference of convex programming relaxation constraint. The lower bound of $\Pi(\mathbf{u})$ is derived as

$$\Pi(\mathbf{u}) \geq \Pi(\mathbf{u}^{(t)}) + \nabla_u \Pi(\mathbf{u}^{(t)})(\mathbf{u} - \mathbf{u}^{(t)}) \triangleq \Pi^{(t)}(\mathbf{u}), \tag{26}$$

$$\Xi(u) - \Pi^{(t)}(\mathbf{u}) \leq 0, \tag{27}$$

where at the t-th iteration, $\Pi(\mathbf{u}^{(t)})$ represents the current value, and the gradient term is computed as

$$\nabla_u \Pi(\mathbf{u}^{(t)})(\mathbf{u} - \mathbf{u}^{(t)}) = \sum_{k\in\mathcal{K}} \sum_{r\in\mathcal{R}} 2(u_{r,k}^{(t)})(u_{r,k} - u_{r,k}^{(t)}). \tag{28}$$

By incorporating the constraint (27) as a penalty term in the objective function and introducing the slack variable $\wp_k^{(t)}$, we effectively address all non-convex terms in the association problem, and the convex approximation of problem (21) is formulated as

$$\max_{\mathbf{\Theta}, \mathbf{u}, \wp} \quad \sum_{k\in\mathcal{K}} 2\sqrt{\varpi_k(1+b_k)}\Re\{\delta_k^\dagger \boldsymbol{\psi}^H \mathbf{g}_{k,k}\} \tag{29a}$$

$$- \sum_{k\in\mathcal{K}} |\delta_k|^2 \left(\sum_{j\in\bar{\mathcal{K}}\setminus k} \boldsymbol{\psi}^H \mathbf{g}_{k,j} \mathbf{g}_{k,j}^H \boldsymbol{\psi} + \sigma^2 \right) - \vartheta^{(t)} \wp_k^{(t)}$$

s.t.

$$\sum_{r\in\mathcal{R}} u_{k,r} \leq R_{connect} + \wp_k^{(t)}, \forall k \in \mathcal{K}, \tag{29b}$$

$$|\psi_{r,n}| \leq 1, \forall r = 1, \ldots R, \forall n = 1, \ldots N, \tag{29c}$$

$$(27), \tag{29d}$$

where $\wp_k^{(t)} = (\Xi(u) - \Pi^{(t)}(u))$ which can be updated by $\wp_k^{(t)} = \max\left(0, \sum_{r=1}^R u_{k,r}^{(t)} - R_{\text{connect}}\right)$, to permit violations. A penalty weight $\vartheta^{(t)}$ is applied to enforce $\wp_k^{(t)} \to 0$, ensuring that constraint (13e) is ultimately satisfied.

D. UAVs' Location Optimization

This section focuses on optimizing the location of the UAVs by decoupling the variables of the UAV for a streamlined process. With fixed $\mathbf{\Theta}, \mathbf{w}, b_k, \delta_k, \mathcal{U}$, we reformulate the channel equations as follows:

$$\begin{aligned} &(\mathbf{g}_{l,k}^H + u_{k,r} \mathbf{g}_{r,k}^H \mathbf{\Theta}_r \mathbf{G}_{l,r}) \mathbf{w}_{l,j} \\ &= \sqrt{d_{lr}^{-2} d_{rk}^{-2}} (\mathbf{g}_{l,k}^H + u_{k,r} \hat{\mathbf{g}}_{r,k}^H \mathbf{\Theta}_r \hat{\mathbf{G}}_{l,r}) \mathbf{w}_{l,j}, \end{aligned} \tag{30}$$

where

$$\hat{\mathbf{G}}_{l,r} = \sqrt{\alpha} \left(\sqrt{\frac{\beta}{\beta+1}} \mathbf{G}_{lr}^{\text{LoS}} + \sqrt{\frac{1}{\beta+1}} \mathbf{G}_{lr}^{\text{NLoS}} \right), \tag{31}$$

$$\hat{\mathbf{g}}_{r,k} = \sqrt{\alpha} \left(\sqrt{\frac{\beta}{\beta+1}} \mathbf{g}_{rk}^{\text{LoS}} + \sqrt{\frac{1}{\beta+1}} \mathbf{g}_{rk}^{\text{NLoS}} \right). \tag{32}$$

Defining $S_{l,k,j} = (\mathbf{g}_{l,k}^H + u_{k,r} \hat{\mathbf{g}}_{r,k}^H \mathbf{\Theta}_r \hat{\mathbf{G}}_{l,r}) \mathbf{w}_{l,j}$, we simplify

$$(\mathbf{g}_{l,k}^H + u_{k,r} \mathbf{g}_{r,k}^H \mathbf{\Theta}_r \mathbf{G}_{l,r}) \mathbf{w}_{l,j} = \sqrt{d_{lr}^{-2} d_{rk}^{-2}} S_{l,k,j}. \tag{33}$$

The AP-RIS and user-RIS links depend on RIS's location, making optimization problem complex. To manage this, we adopt a local area optimization approach, restricting RIS movement within a small threshold Δ to maintain a near-constant channel model. To maximize the weighted transmission rate, we define the optimization problem as follows:

$$\max_{\mathbf{q}} \sum_{k\in\mathcal{K}} \varpi_k \Upsilon_k \tag{34}$$

subject to the constraint:

$$\|\mathbf{q}-\mathbf{q}^{(t)}\| \le \Delta, \quad \mathbf{q}\in E. \tag{35}$$

The rate function $\tilde{R}_k$ is given by

$$\tilde{\Upsilon}_k = \log_2\left(\sum_{l\in L}\sum_{j\in\mathcal{K}} \frac{S_{l,k,j}S_{l,k,j}^H}{d_{lr}^2 d_{rk}^2} + \sigma^2\right) - \log_2\left(\sum_{l\in L}\sum_{j\in\bar{\mathcal{K}}\setminus k} \frac{S_{l,k,j}S_{l,k,j}^H}{d_{lr}^2 d_{rk}^2} + \sigma^2\right).$$

However, $\tilde{\Upsilon}_k$ is highly nonlinear, complicating direct optimization. To address this, we introduce relaxation variables $X_{l,k}$ and $Y_{l,k}$, and reformulate $\tilde{\Upsilon}_k$ as a concave function as follows:

$$\begin{aligned}\tilde{\Upsilon}_k \ge \tilde{\Upsilon}_k^* = {}& \log_2\left(\sum_{l\in L}\sum_{j\in\mathcal{K}} \frac{S_{l,k,j}S_{l,k,j}^H}{X_{l,k}} + \sigma^2\right) \\ & - \frac{1}{\ln(2)}\sum_{l\in L}\sum_{j\in\mathcal{K}} \frac{S_{l,k,j}S_{l,k,j}^H(X_{l,k}-X_{l,k}^{(t)})}{X_{l,k}^{(t),2}} \\ & \times\left(\sum_{l\in L}\sum_{j\in\mathcal{K}} \frac{S_{l,k,j}S_{l,k,j}^H}{X_{l,k}} + \sigma^2\right)^{-1} \\ & - \log_2\left(\sum_{l\in L}\sum_{j\in\bar{\mathcal{K}}\setminus k} \frac{S_{l,k,j}S_{l,k,j}^H}{Y_{l,k}} + \sigma^2\right).\end{aligned} \tag{36}$$

For convexity, the constraint $X_{l,k} \ge d_{rk}^2 d_{lr}^2$ must hold. By using the SCA method, we approximate

$$\begin{aligned} d_{rk}^2 d_{lr}^2 \le {}& \frac{1}{2}\left[(d_{rk}^2+d_{lr}^2)^2 - (d_{rk}^{(t)})^4\right] \\ & - 2(d_{rk}^{(t)})^2(\mathbf{q}-\boldsymbol{\chi}_k^K)^T\mathbf{q}-\mathbf{q}^{(t)}) \\ & - 2(d_{rk}^{(t)})^2(\mathbf{q}-\boldsymbol{\chi}_l^L)^T(\mathbf{q}-\mathbf{q}^{(t)}) \\ & = \Im_1(l,k).\end{aligned} \tag{37}$$

Thus, by leveraging SCA, we transform the problem into a convex optimization framework, ensuring an efficient solution. To ensure a lower bound on $\tilde{\Upsilon}_k$, the relaxation variable $Y_{l,k}$ must satisfy:

$$Y_{l,k} \le d_{rk}^2 d_{lr}^2. \tag{38}$$

Since $d_{rk}^2 d_{lr}^2$ is a product of two convex terms, its upper approximation is formulated as:

$$\begin{aligned} d_{rk}^2 d_{lr}^2 \ge {}& \frac{1}{2}\left(\left(d_{rk}^{(t)2}+d_{lr}^{(t)2}\right)^2 - \left(d_{rk}^{(t)4}+d_{lr}^{(t)4}\right)\right) \\ & + 2\left((d_{rk}^{(t)2}+d_{lr}^{(t)2})(\mathbf{q}^{(t)}-\boldsymbol{\chi}_k^K)^T(\mathbf{q}-\mathbf{q}^{(t)})\right) \\ & + 2\left((d_{rk}^{(t)2}+d_{lr}^{(t)2})(\mathbf{q}^{(t)}-\boldsymbol{\chi}_l^L)^T(\mathbf{q}-\mathbf{q}^{(t)})\right) \\ & = \Im_2(l,k).\end{aligned} \tag{39a}$$

When $\Im_2(l,k) \ge Y_{l,k}$, the constraint $Y_{l,k} \le d_{rk}^2 d_{lr}^2$ holds, ensuring convexity. Standard convex optimization methods, such as the primal-dual interior-point algorithm, are then applied to solve the problem. The convex approximation of problem (34) is given by

$$\max_{\mathbf{q}} \quad \sum_{k\in\mathcal{K}} \tilde{\Upsilon}_k^* \tag{40a}$$

$$\text{s.t.} \tag{40b}$$

$$\|\mathbf{q}-\mathbf{q}^{(t)}\| \le \Delta, \quad \mathbf{q}\in E, \tag{40c}$$

$$X_{l,k} \ge \Im_1(l,k), \tag{40d}$$

$$Y_{l,k} \le \Im_2(l,k). \tag{40e}$$

The proposed alternating optimization algorithm is outlined in Algorithm 1.

Algorithm 1 Alternating Optimization for Problem (13)

Initialize $t=0$, $\mathbf{g}$, $\boldsymbol{\Theta}$, $\mathbf{G}$, $\mathbf{w}$, $\mathbf{q}$, $\mathcal{U}$.
repeat
  $t = t+1$
  if $\max\left\|\mathcal{U}^{(t)}-\mathcal{U}^{(t-1)}\right\| > \epsilon$ **then**
    Update $\mathcal{U}$, $\wp_k^{(t)}$ by solving (29)
  end if
  Update b_k
  Update δ_k^*, by (17)
  Update $\mathbf{w}$, by (19)
  Update $\boldsymbol{\Theta}$, by (29)
  Update $\mathbf{q}$, by (40)
  Compute $\Upsilon^{(t)}$.
until $|\Upsilon^{(t)}-\Upsilon^{(t-1)}| \le \epsilon$
return $\mathcal{U}^*$, $\mathbf{w}^*$, $\boldsymbol{\Theta}^*$, $\mathbf{q}^*$, Υ^*

V. SIMULATION RESULTS

This section presents the simulation outcomes to evaluate the performance of CF-ISAC system with URISs. In the considered setup, there are $L=4$ distributed APs, $K=4$ UEs, $R=4$ RISs, and $F=4$ SRs. The users and sensing target each have a single antenna, while both the APs and SRs are equipped with 4 antennas. Each RIS is composed of $N=8$ passive reflecting elements. The maximum transmit power at each AP is limited to $P_l^{\max}=1\,\text{W}$, and the noise power is set to $\sigma^2=-110\,\text{dBm}$. The minimum SNR threshold for sensing are set at $\gamma_{th}^{sens}=0$ dB. All APs, users, and SRs are uniformly distributed within a circular region with a radius of 1 km.

Fig. 2 shows the convergence behavior of Algorithm 1. The Algorithm typically converges to the optimal value after about

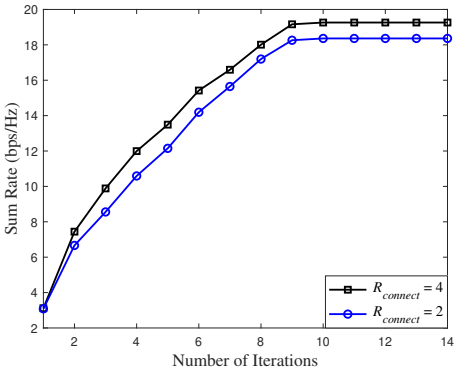

Fig. 2. Convergence behavior of Algorithm 1.

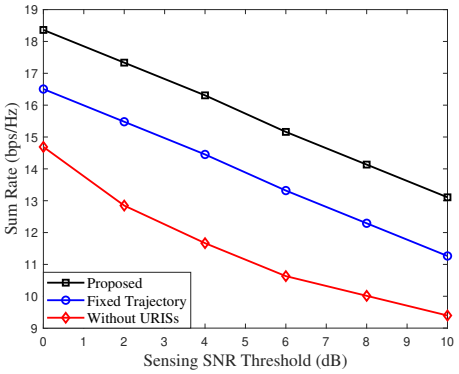

Fig. 3. The effect of sensing SNR threshold on the weighted sum rate.

ten iterations, highlighting the efficiency of the proposed method. Furthermore, as $R_{connect}$ increases, the weighted sum rate improves because each user can be paired with more RISs.

Fig. 3 illustrates the trade-off between communication performance and sensing requirement. It is clear that the weighted sum rate for all cases decreases as the sensing SNR threshold increases. This happens because a stricter sensing constraint requires more power for the sensing beamformer, leaving less power available to optimize the communication beamformer for maximizing the weighted sum rate. Besides, our proposed scheme considerably outperforms the CF-ISAC systems with fixed UAV trajectory and without URISs, thus confirming the benefits of deploying and optimizing URISs' location.

VI. Conclusion

In this paper, we proposed an efficient optimization framework for the URISs-assisted CF-ISAC system. The objective is to maximize the weighted sum rate by jointly optimizing APs' transmit beamforming, RISs' phase shifts, user-RIS association, and UAVs' locations. This is formulated as a non-convex optimization problem, which is addressed using an efficient alternating optimization algorithm. Simulation results demonstrate significant performance improvements, showcasing the potential of our proposed approach for future RIS-mounted UAVs assisted CF-ISAC applications. Future work may consider imperfect CSI modeling, hybrid/active RIS architectures, and learning-based optimization for next-generation CF-ISAC performance.

Acknowledgments

This work was supported by the Canada Excellence Research Chair (CERC) Program CERC-2022-00109 and in part by NSERC Discovery Grant Program RGPIN-2025- 04941.

References

[1] Q. Xue *et al.*, "A survey of beam management for mmWave and THz communications towards 6G," *IEEE Commun. Surv. Tutor.*, vol. 26, no. 3, pp. 1520–1559, 3rd Quart. 2024.

[2] Z. Wei *et al.*, "Integrated sensing and communication signals toward 5G-A and 6G: A survey," *IEEE Internet Things J.*, vol. 10, no. 13, pp. 11 068–11 092, Jul. 2023.

[3] S. Lu *et al.*, "Integrated sensing and communications: Recent advances and ten open challenges," *IEEE Internet Things J.*, vol. 11, no. 11, pp. 19 094–19 120, Jun. 2024.

[4] S. Ghosh *et al.*, "On the performance of rate splitting multiple access for ISAC in device-to-multi-device IoT communications," *IEEE Trans. Cogn. Commun. Netw.*, vol. 11, no. 1, pp. 333–348, Aug. 2024.

[5] Z. Hong, S. Sugiura, C. Xu, and L. Hanzo, "Cooperative ISAC networks: Performance analysis, scaling laws and optimization," *IEEE Trans. Wirel. Commun.*, vol. 24, no. 2, pp. 877–892, Feb. 2025.

[6] J. M. Mateos-Ramos *et al.*, "Model-driven end-to-end learning for integrated sensing and communication," in *Proc. IEEE Int. Conf. Commun. (ICC)*, Rome, Italy, Oct. 2023, pp. 5695–5700.

[7] A. A. Salem *et al.*, "Integrated cooperative sensing and communication for RIS-enabled full-duplex cell-free MIMO systems," *IEEE Trans. Commun.*, pp. 1–1, Nov. 2024.

[8] Z. Behdad *et al.*, "Power allocation for joint communication and sensing in cell-free massive MIMO," in *Proc. IEEE GLOBECOM*, Rio de Janeiro, Brazil, Dec. 2022, pp. 4081–4086.

[9] H. Zhao *et al.*, "Joint beamforming design for RIS-aided secure integrated sensing and communication systems," *IEEE Commun. Lett.*, vol. 27, no. 11, pp. 2943–2947, Nov. 2023.

[10] S. Shakoor, Q. N. Le, E.-K. Hong, B. Canberk, and T. Q. Duong, "Integrated sensing and communications for reconfigurable intelligent surface-aided cell-free networks," *IEEE Commun. Lett.*, vol. 29, no. 6, pp. 1275–1279, Jun. 2025.

[11] H. Luo *et al.*, "Joint beamforming design for RIS-assisted integrated sensing and communication systems," *IEEE Trans. Veh. Technol.*, vol. 71, no. 12, pp. 13 393–13 397, Dec. 2022.

[12] D. Bao and R. Guo, "A dual function intelligent reflecting surface in integrated radar communication system," *IEEE Trans. Intell. Transp. Syst.*, vol. 26, no. 3, pp. 3471 – 3481, Jan. 2025.

[13] S. Shakoor, Q. N. Le, L. D. Nguyen, K. Singh, O. A. Dobre, and T. Q. Duong, "Max-min fairness in active aerial reconfigurable intelligent surface-aided ISAC network," *IEEE Trans. Cogn. Commun. Netw.*, vol. 11, no. 5, pp. 2910–2922, Oct. 2025.

[14] X. Yuan, Y. Hu, J. Zhang, and A. Schmeink, "Joint user scheduling and UAV trajectory design on completion time minimization for UAV-aided data collection," *IEEE Trans. Wireless Commun.*, vol. 22, no. 6, pp. 3884–3898, Jun. 2022.

[15] D. Tyrovolas *et al.*, "Energy-aware trajectory optimization for UAV-mounted RIS and full-duplex relay," *IEEE Internet Things J.*, vol. 11, no. 13, pp. 24 259 – 24 272, April. 2024.

[16] M. A. Mohsin *et al.*, "Deep reinforcement learning optimized intelligent resource allocation in active RIS-integrated TN-NTN networks," in *Proc. IEEE Wireless Commun. Netw. Conf*, Milan, Italy, Mar. 2025, pp. 1–7.

[17] Y. Song *et al.*, "Joint beamforming and user association design in active RIS-aided cell-free URLLC system," in *16th IEEE WCSP*, Hefei, China, Oct. 2024, pp. 242–247.

[18] A. A. Nasir, "Joint users' secrecy rate and target's sensing SNR maximization for a secure cell-free ISAC system," *IEEE Commun. Letters*, vol. 28, no. 7, pp. 1549–1553, Jul. 2024.

[19] K. Shen and W. Yu, "Fractional programming for communication systems—Part I: Power control and beamforming," *IEEE Trans. Signal Process.*, vol. 66, no. 10, pp. 2616–2630, May 2018.